

Improved open-circuit voltage of benzodithiophene based polymer solar cells using bulky terthiophene side group



Qian Liu^{a,b}, Xichang Bao^b, Liangliang Han^b, Chuantao Gu^b, Meng Qiu^b, Zhengkun Du^b, Ruiying Sheng^{a,b}, Mingliang Sun^{a,*}, Renqiang Yang^{b,**}

^a Institute of Materials Science and Engineering, Ocean University of China, Qingdao, Shandong 266100, China.

^b CAS Key Laboratory of Bio-based Materials, Qingdao Institute of Bioenergy and Bioprocess Technology, Chinese Academy of Sciences, Qingdao, Shandong 266101, China

ARTICLE INFO

Article history:

Received 1 December 2014

Received in revised form

12 February 2015

Accepted 21 February 2015

Available online 13 March 2015

Keywords:

Polymer solar cells

Open-circuit voltage

Benzodithiophene

Terthiophene side chain

ABSTRACT

Terthiophene, including one α - α and one branching α - β connection of the thiophene units, is introduced as benzodithiophene (BDT) side chain to build a novel two-dimensional (2D) conjugated BDT block. By copolymerizing this BDT block with three electron acceptors (DTTz (bis(thiophene-2-yl)-tetrazine), DPP (diketopyrrolopyrrole), DTffBT (4,7-bis(4-hexylthienyl)-5,6-difluoro-2,1,3-benzothiadiazole)) and one electron donor (TTT (2,5-Di(2-thienyl)thiophene)), four terthiophene side-chained benzodithiophene based copolymers were synthesized. Due to the difference in electron affinity among DTTz, DPP, DTffBT and TTT, these four polymers show different UV-vis absorption spectra and optical band gaps (1.3–2.0 eV), while fortunately they all remain deep highest occupied molecular orbital (HOMO) energy levels (−5.3 to 5.6 eV) which is very favorable to high open-circuit voltage (V_{oc}) polymer solar cells (PSCs). By comparing the photovoltaic properties with polymers which have same backbone but do not have the bulky 2D side group in the literatures, our polymer solar cells devices show higher V_{oc} . Especially for PQ3 (a copolymer of benzodithiophene and diketopyrrolopyrrole), the donor photon energy loss ($E_g - eV_{oc}$) is 0.51 eV which is almost the lowest value achieved by the researchers. It can be concluded that: the bulky terthiophene side group helps to improve V_{oc} of the PSCs devices. The overall performance of solar cells devices is correlated with the molecule conformation, polymer hole mobility and polymer/PCBM blend film morphology.

© 2015 Elsevier B.V. All rights reserved.

1. Introduction

Polymer solar cells (PSCs) have attracted considerable interests due to their unique advantages in the development of renewable energy resources, such as low cost, light weight, flexibility and easy processability [1]. Bulk heterojunction (BHJ) polymer solar cells device architecture, based on a variety of blends of electron-donating semiconductor polymers and electron-accepting fullerene derivatives, has been proved to be the most efficient devices structure [2–5]. Among various types of semiconducting polymers, the benzo[1,2-*b*:4,5-*b'*]dithiophene (BDT) based polymers exhibited promising photovoltaic properties, since BDT unit possesses its special merits. Firstly, BDT has a large planar conjugated structure and easily forms π - π stacking, which improves polymer mobility [6,7]. Secondly, there

is small steric hindrance between BDT and adjacent units, as 4,9-bis-substituted-BDT has no substituent on 1,3,5 and 7 positions, which makes BDT an ideal conjugated unit for photovoltaic material. Thirdly, starting from 4,8-dihydrobenzo[1,2-*b*:4,5-*b'*]dithiophene-4,8-dione, it is very easy to attach different substituents to the central benzene core of BDT by nucleophilic addition which can tune the optical-electronic properties of resultant polymers.

In 2008, Hou et al. synthesized the 4,8-bisalkoxy-BDT monomer and prepared eight photovoltaic polymers by copolymerizing this BDT monomer with different units [8]. After that, lots of new alkoxy-BDT based polymers have been designed, synthesized and applied for PSCs within the past five years [9–12]. Many milestone PCE achievements in recent years are also based on BDT polymers [13–17]. According to the reported works, efficient photovoltaic materials can be obtained by copolymerizing BDT units with other types of conjugated building blocks [18]. For example, 8–9% PCEs have been achieved by the BDT with thieno[3, 4-*b*]thiophene (TT) copolymers [13–16], the BDT with TPD copolymers [17], etc.

* Corresponding author. Tel.: +86 532 66781690; fax: +86 532 66781927.

** Corresponding author. Tel.: +86 532 80662700; fax: +86 532 80662778.

E-mail addresses: mlsun@ouc.edu.cn (M.-A. Sun), yangrq@qibebt.ac.cn (R. Yang).

Therefore, how to further improve photovoltaic properties of the BDT-based polymers is a very important topic for molecular engineering.

Li's group developed the concept of two-dimensional conjugated polythiophenes (2D-PTs) [19]. Recently, Li et al. summarized the progress of the 2D-PTs in a review paper [20]. They found that, it is a very effective method to enhance the open-circuit voltage (V_{oc}) by using the 2D-structure. On this basis, Yang and Hou et al. introduced 2,4-diocetylthienyl substituent onto BDT unit and constructed the first 2D-conjugated BDT polymer [21], named as PBDTTBT-T. Although the steric hindrance caused by the alkyls at 4-position of the thiophene unit is too strong to get effective conjugated effect of the side groups, PBDTTBT-T showed a high V_{oc} of 0.92 V, thus resulting in one of the outstanding photovoltaic data. Then, many pairs of BDT polymers, which are substituted by alkoxy or conjugated side groups, were designed and synthesized [22–28]. By comparing the photovoltaic properties of each pair of polymers, the conclusion is drawn that once the substituents on BDT are changed from alkoxy chains to conjugated side groups, their HOMO levels are reduced and thus the V_{oc} of corresponding PSCs device is increased. So far, we can say that, for all the materials based on BDT, it is a certain thing to increase their V_{oc} by introducing the conjugated side chain substituent [29].

Terthiophene, including one α - α and one branching α - β connection of the thiophene units, can be used to directly allow selective reactions at the inner free α -position, and the other two outer α -positions can connect different functional groups by electrophilic reactions. Janssen et al. designed and synthesized two series of oligothiophene dendrimers based on terthiophene unit with silylated and nonsubstituted two outer α -positions [30]. Solution-processed bulk heterojunction photovoltaic cells based on these two materials exhibited a high V_{oc} of 1.0 V which showed that terthiophene unit is an excellent group for organic electronics.

Previously, our research group has reported one new 2D BDT building block, bulky terthiophene-substituted BDT (3TC12BDT). Polymer based on this building block and 4,7-di(thiophen-2-yl)-benzo[c] [1, 2, 5] thiadiazole showed a PCE of 3.57% [31]. In this work, we selected three other acceptors and one donor unit, DTTz [32], DPP [33], DTffBT [34] and TTT [35] to copolymerize with 3TC12BDT forming four novel polymers. The PSCs devices based on these four polymers with our new bulky side chain (terthiophene) show high V_{oc} compared with those polymers without 2D side chain or even those with typically 2D side chain (alkylthienyl).

2. Experimental section

2.1. Materials

All reagents and chemicals were purchased from commercial sources (Acros, Aldrich, Alfa, J&K) and used as received without further purification unless otherwise noted. 3TC12BDTBr was synthesized according to our previously published procedures [31]. DTTz [32], DPP [33] and TTT [35] have been reported in the corresponding literatures. DTffBT was bought from Derthon Optoelectronic Materials Sciences & Technology Co., LTD. All reactions were conducted under purified argon atmosphere. Tetrahydrofuran (THF) and toluene were distilled from sodium/benzophenone. *N,N*-Dimethylformamide (DMF) was distilled from calcium hydride.

2.2. Instrumentation

^1H and ^{13}C NMR spectra were recorded using the Bruker Avance-III 600MHz spectrometer at 25 °C in CDCl_3 . The number-average (M_n) and weight-average (M_w) molecular weights of polymers were determined by gel permeation chromatography (GPC) on a HLC-8320

instrument, using THF as eluting solvent and polystyrene as standard. The thermal gravimetric analysis (TGA) was made using a SDT Q600 instrument and operated under a nitrogen atmosphere. The Ultra-violet-visible (UV-vis) absorption spectra were measured by a Hitachi U-4100 spectrometer. Cyclic voltammetry (CV) was performed on a CHI660D electrochemical workstation with a glassy carbon working electrode, a platinum wire counter electrode and Ag/AgCl reference electrode in a solution of Bu_4NPF_6 (0.1 M) in acetonitrile at a scan rate of 50 mV/s. The XRD samples of the polymer only and blend films with PCBM were prepared by casting the corresponding solutions in o-DCB (ortho-dichlorobenzene) in a concentration of 24 mg/ml. AFM studies were carried out on a VEECO-dimension 5000 scanning probe microscope.

2.3. Preparation of solar cell devices

Solar cells devices were fabricated with the structure of ITO/PEDOT:PSS/Polymer:PCBM/Ca/Al. Glass substrates coated with ITO (170 nm) were patterned using standard photolithography. The substrates were cleaned by ITO lotion (commercially available), distilled water, acetone and isopropyl alcohol in ultrasonication bath for 30 min. The substrates were subjected to oxygen plasma treatment for 3 min twice prior to use. After that, poly(3,4-ethyl-enedioxythiophene):poly(styrenesulfonate) (PEDOT:PSS) was spin coated on the substrates (4000 rpm, 20 s). The thickness of the PEDOT:PSS layer was ~30 nm, as determined by a Dektak 150 surface profilometer. The substrates were annealing at 160 °C for 30 min under a nitrogen atmosphere. Polymer:PCBM blends (1:1 to 1:4) were in o-DCB with a total blend concentration of 24 mg/ml which were spin coated on to the PEDOT:PSS treated substrates. Films of 20 nm Ca and 100 nm Al were thermally evaporated onto the substrates through a shadow mask to obtain the solar cell devices. *J-V* testing was carried out under a controlled nitrogen atmosphere using a Keithley 2420 source measurement unit under simulated 100 mW/cm² (AM 1.5G) irradiation from a Newport solar simulator. The active area of the devices was 0.1 cm².

2.4. Space Charge Limited Current (SCLC)

ITO/PEDOT:PSS/Polymer:PCBM substrate was prepared as solar cells devices and then Au (100 nm thickness) was thermally evaporated on the substrates through a shadow mask to obtain the devices. *J-V* testing was carried out under a controlled nitrogen atmosphere using a Keithley 2420 source measurement unit. The active area of the devices was 0.1 cm². The active layer film thickness was measured using a Dektak 150 surface profilometer. The SCLC mobilities μ were extracted using the standard trap-free SCLC transport equation:

$$J = \frac{9}{8} \epsilon_r \epsilon_0 \mu \frac{U^2}{d^3}$$

where ϵ_r is the relative dielectric constant, ϵ_0 is the vacuum permeability, U is the applied voltage, and d is the device thickness.

2.5. Synthesis of the monomer and polymers

The monomer 3TC12BDTBr was synthesized according to our reported procedures [31].

2.5.1. Synthesis of 3TC12BDTSn

3TC12BDTBr (3.03 g, 2.0 mmol) and 80 mL of THF were added into a 200 mL flask under an inert atmosphere. The solution was cooled down to 0 °C by an ice-water bath, and 5.0 mmol of n-butyllithium (3.13 mL, 1.6 M in n-hexane) was added dropwise. After being stirred

at 0 °C for 2 h, a great deal of yellow solid precipitate appeared in the flask. Then, 5.4 mmol of trimethyltin chloride (5.4 mL, 1 M in n-hexane) was added in one portion, and the reactant turned to clear rapidly. The cooling bath was removed, and the reactant was stirred at ambient temperature overnight. Then, it was poured into 100 mL of cool water and extracted with ether three times. The organic layer was washed by water twice and then dried by anhydrous MgSO₄. After removing solvent under vacuum, the residue was recrystallized by isopropanol twice and used in next step for the copolymerization (2.6 g, 1.55 mmol, Yield = 77.5%). ¹H NMR (600 MHz, CDCl₃): δ (ppm) 7.78 (s, 2H), 7.53 (s, 2H), 7.07 (d, *J* = 3.6 Hz, 2H), 7.00 (d, *J* = 3.6 Hz, 2H), 6.73 (d, *J* = 3.0 Hz, 2H), 6.71 (d, *J* = 3.6 Hz, 2H), 2.80 (m, 8H), 1.68 (m, 8H), 1.38–1.26 (m, 72H), 0.88 (m, 12H), 0.43 (s, 18H). ¹³C NMR (151 MHz, CDCl₃): δ (ppm) 147.77, 146.28, 143.31, 143.11, 138.49, 137.38, 134.97, 132.16, 132.15, 132.10, 130.94, 130.46, 127.81, 126.28, 124.26, 124.09, 121.57, 31.94, 31.65, 31.63, 31.60, 30.24, 30.17, 29.70, 29.69, 29.67, 29.62, 29.42, 29.40, 29.38, 29.16, 29.15, 26.93, 22.71, 14.13, –8.19.

2.5.2. General procedure for the synthesis of copolymers

These four polymers were synthesized with the same procedure of coupling dibromide compounds with bis(triethylstannyl)-substituted compounds. 0.2 mmol of dibromide compound and 0.2 mmol of bis(triethylstannyl)-substituted compound were mixed in 8 mL of toluene and 2 mL of DMF. After being purged by argon for 30 min, 5.5 mg of Pd₂(dba)₃ and 14.6 mg of P(*o*-tol)₃ were added as catalyst. Then the mixture was purged by argon for another 30 min and heated up to 100 °C and kept for 36 h. The reactant was cooled down to room temperature, poured into MeOH (200 mL), and then filtered through a Buchner funnel. The crude product was then subjected to Soxhlet extraction with methanol, hexane, and chloroform. The polymer solution was concentrated and was poured into MeOH. Then the precipitate was collected and dried under vacuum overnight.

PQ1 (265 mg, Yield = 83%): ¹H NMR (600 MHz, CDCl₃): δ (ppm) 7.99–7.43 (br, 4H), 7.22–6.20 (br, 12H), 3.01–2.64 (s, 8H), 1.89–1.58 (s, 8H), 1.50–1.03 (s, 72H), 0.96–0.75 (s, 12H).

PQ2 (250 mg, Yield = 78%): ¹H NMR (600 MHz, CDCl₃): δ (ppm) 7.75–7.29 (br, 4H), 7.22–6.14 (br, 14H), 3.16–2.42 (s, 8H), 2.01–1.60 (s, 8H), 1.51–1.04 (s, 72H), 0.92–0.77 (s, 12H).

PQ3 (342 mg, Yield = 91%): ¹H NMR (600 MHz, CDCl₃): δ (ppm) 8.00–7.28 (br, 4H), 7.22–6.25 (br, 12H), 3.01–2.67 (s, 10H), 1.88–1.62 (s, 12H), 1.53–1.14 (s, 88H), 1.00–0.86 (s, 24H).

PQ4 (305 mg, Yield = 82%): ¹H NMR (600 MHz, CDCl₃): δ (ppm) 8.71–7.33 (br, 4H), 7.18–6.18 (br, 10H), 3.24–2.17 (s, 12H), 2.00–1.62 (s, 12H), 1.52–1.03 (s, 84H), 1.00–0.68 (s, 18H).

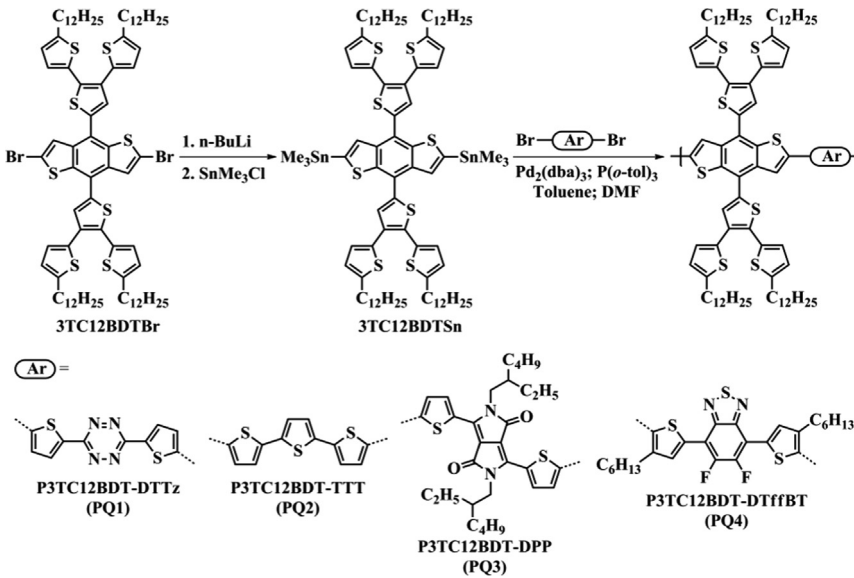
3. Results and discussion

3.1. Synthesis and characterization

Four alternating copolymers have been synthesized by polymerizing our new synthesized benzodithiophene building block containing bulky thiophene side chain substitute with four other building blocks, DTTz, TTT, DPP and DTffBT in good yields (around 80%). The general synthetic route for 3TC12BDTSn and the copolymers is outlined in **Scheme 1**. All the polymers show excellent solubility at room temperature in common organic solvents such as chloroform (CHCl₃), tetrahydrofuran (THF), toluene, chlorobenzene and *o*-dichlorobenzene (*o*-DCB). The molecular weight (*M_n* and *M_w*) and polydispersity (PDI) were measured by gel permeation chromatography (GPC) using THF as the eluent and polystyrenes as the internal standards, and the results are listed in **Table 1**. The *M_n* of PQ1, PQ2, PQ3, PQ4 is 34.7, 33.9, 48.2, 32.6 kDa, and PDI is 1.76, 2.44, 1.43, 1.58, respectively.

3.2. Thermal properties

Thermal properties of the polymers were investigated using thermogravimetric analysis (TGA). All polymers exhibited good thermal stability (**Fig. 1**). The decomposition temperature (*T_d*) of PQ1, PQ2, PQ3 and PQ4 determined at 5% weight loss was 329, 445, 420 and 447 °C, respectively. Interestingly, a plateau at 5% weight loss from 329 to 439 °C appears in the TGA plot of PQ1. It is reasonable for the assumption that the *T_d* of 329 °C resulted from the tetrazine unit because its mass fraction in the repeated unit is definitely 5% which agree with the experimental data. Similar phenomenon was also observed from other tetrazine containing polymers [32]. In addition, the plateau also indicated that the decomposition of tetrazine did not affect the thermal properties of residual fragments.



Scheme 1. Synthetic route of the polymers (PQ1–PQ4).

3.3. UV-vis absorption properties

The Ultraviolet-visible (UV-vis) absorption spectra of these four polymers in chloroform solutions and thin films are shown in Fig. 2

Table 1
Molecular weights and thermal properties of the polymers.

Polymers	Yield (%)	M_n (kDa)	M_w (kDa)	PDI ^a	T_d ^b (°C)
PQ1	83	34.7	61.1	1.76	329
PQ2	78	33.9	82.7	2.44	445
PQ3	91	48.2	68.9	1.43	420
PQ4	82	32.6	51.6	1.58	447

^a PDI = M_w/M_n .

^b The decomposition temperature (T_d) was taken as 5% weight loss under nitrogen.

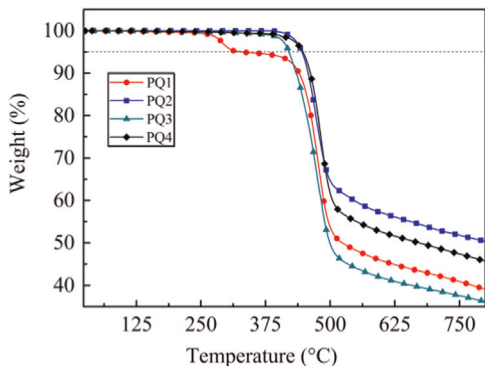


Fig. 1. TGA plots of the four copolymers with a heating rate of 10 °C/min under inert atmosphere.

(a) and (b), respectively. The four polymers show much different absorption properties. As listed in Table 2, the absorption peaks of PQ1, PQ2, PQ3, and PQ4 are located at 532, 567, 757, and 585 nm in solution, respectively which are due to the $\pi-\pi$ transition along the conjugated polymer backbone [36,37]. From solution state to solid film, PQ1, PQ2, and PQ4 exhibited a red-shift (11 nm for PQ1, 17 nm for PQ2, 16 nm for PQ4), while PQ3 did not show any red-shift. The absence of a red-shift was attributed to the fact that the PQ3 polymer has a rigid rod conformation both in solution and thin films [38,39]. The red-shift of PQ1, PQ2, and PQ4 indicated more structural organization and ordered packing which enhanced the aggregation of the polymer in thin films compared to that of the solution. For PQ2, we can observe an obvious increase in the intensity of the shoulder peak from solution (533 nm) to solid state (547 nm) which could be due to the enhanced intermolecular interactions in the solid state [25,40]. The onset wavelength (λ_{onset}) of the four polymer films are 632, 628, 962, and 716 nm for PQ1, PQ2, PQ3, and PQ4, respectively, from which the optical band gaps (E_g) were calculated according to $E_g = 1240/\lambda_{\text{onset}}$ and the results are listed in Table 2. UV-vis absorption of the polymer is not affected by the deposition conditions and thermal annealing process (Figs. S1–S3). The absorption coefficients of these four polymer are around $2\text{--}5 \times 10^4 \text{ cm}^{-1}$ (Fig. S4).

3.4. Electrochemical properties

The electrochemical cyclic voltammetry was performed for determining the highest occupied molecular orbital (HOMO) and the lowest unoccupied molecular orbital (LUMO) energy levels of the conjugated polymers [41]. The HOMO energy levels were determined by measuring the onset oxidation potential ($E_{\text{ox, onset}}$) of the polymer films. To obtain the oxidation potentials, the reference electrode was calibrated using ferrocene/ferrocenium (Fc/Fc⁺),

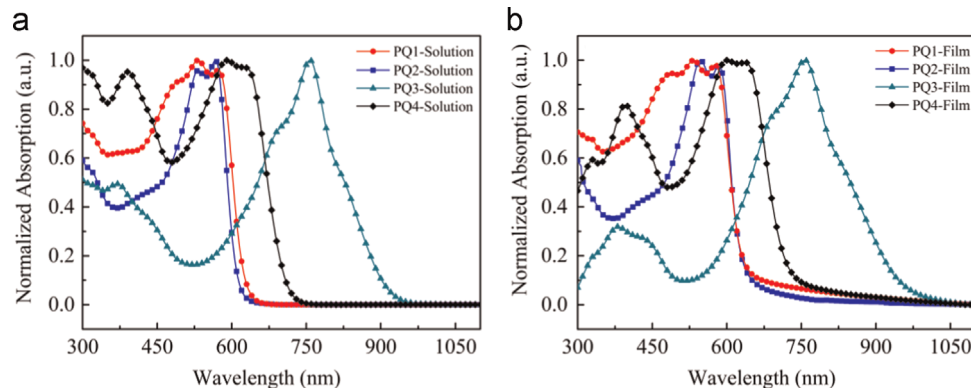


Fig. 2. UV-vis absorption spectra of polymers in (a) chloroform and (b) as thin solid film.

Table 2
Optical properties and electronic energy levels of the polymers.

Polymers	$\lambda_{\text{max}}^{\text{a}}$ (nm)	$\lambda_{\text{max}}^{\text{b}}$ (nm)	$\lambda_{\text{onset}}^{\text{c}}$ (nm)	E_g^{d} (eV)	$E_{\text{ox, onset}}^{\text{e}}$ (V)	HOMO ^f (eV)	LUMO ^g (eV)	HOMO ^h	LUMO ^h
PQ1	532	533	632	1.96	1.20	-5.61	-3.65	-5.04	-2.57
PQ2	567	584	628	1.97	0.87	-5.28	-3.31	-4.87	-2.05
PQ3	757	757	962	1.29	0.90	-5.31	-4.02	-4.84	-2.59
PQ4	585	601	716	1.73	1.18	-5.59	-3.86	-4.95	-2.73

^a Absorption peak measured in chloroform solution.

^b Absorption peak measured in thin film.

^c The lambda offset equaled the intersection formed by the linear extrapolation of UV-vis absorption spectrum and the background signal.

^d Calculated from the empirical equation: $E_g = 1240/\lambda_{\text{onset}}$.

^e The $E_{\text{ox, onset}}$ equaled the intersection formed by the linear extrapolation of CV of spectrum and the background signal.

^f Estimated from the onset of oxidation wave of CV.

^g LUMO = $E_g + \text{HOMO}$.

^h DFT data.

which had a redox potential with an absolute energy level of -4.80 eV in a vacuum; the potential of this external standard under the same conditions was 0.39 V vs Ag/Ag⁺. Fig. 3 shows the cyclic voltammograms of the copolymer films on Pt disk electrode in 0.1 mol/L Bu₄NPF₆ acetonitrile solution. The onset oxidation potential ($E_{\text{ox},\text{onset}}$) of PQ1, PQ2, PQ3 and PQ4 are 1.20 , 0.87 , 0.90 , 1.18 V vs Ag/Ag⁺, respectively. From $E_{\text{ox},\text{onset}}$ of the polymers, HOMO energy levels as well as LUMO energy levels of the polymers were calculated according to the equations:

$$\text{HOMO} = -e(E_{\text{ox},\text{onset}} + 4.41)(\text{eV})$$

$$\text{LUMO} = \text{HOMO} + E_g(\text{eV})$$

where the unit of $E_{\text{ox},\text{onset}}$ is V vs Ag/Ag⁺. The results of the electrochemical measurements are listed in Table 2. The HOMO energy levels of PQ1, PQ2, PQ3 and PQ4 are -5.61 , -5.28 , -5.31 , -5.59 eV, respectively. The LUMO energy levels of PQ1, PQ2, PQ3 and PQ4 are -3.65 , -3.31 , -4.02 , -3.86 eV, respectively. The LUMO energy levels of the polymers decreased significantly with the increase of the electron-withdrawing ability of the copolymerization unit from TTT to DTTz, DTffBT and DPP. All the polymers show relatively deep HOMO energy levels which is desirable for high open circuit voltage (V_{oc}) of the PSCs devices, since V_{oc} is related to the

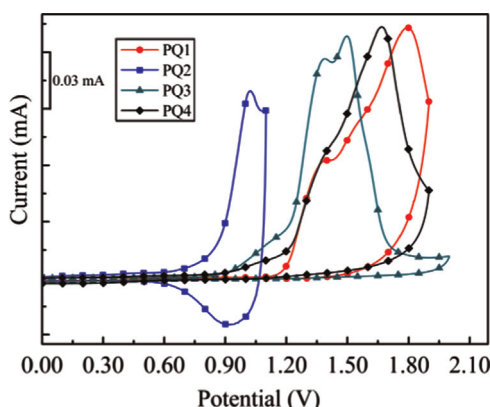


Fig. 3. Cyclic voltammograms of the copolymer films.

difference of the LUMO of the electron acceptor (typically PCBM) and the HOMO of the electron donor polymer [42].

3.5. Density function theory (DFT) calculation

In order to further understand the electronic properties of the four polymers, the molecular geometries and the electron density states distribution of the four polymers were simulated by density functional theory (DFT). The DFT calculations were performed using Gaussian 09 with a hybrid B3LYP correlation functional [43,44] and a split valence 6-31G* basis set [45]. Oligomers containing only one repeating unit are taken as a model for the calculations. Methyl is used instead of long side chains. The optimized molecular geometries of the models and their calculated HOMO and LUMO frontier orbitals are depicted in Fig. 4 and Table 2. For PQ2 and PQ4, the distributions of HOMO and LUMO frontier orbitals propose that there is an effective intra-molecular charge transfer occurring. While for PQ1 and PQ3, the distributions of HOMO and LUMO frontier orbitals are not continuous which may lead to poor intra-molecular charge transfer and decrease the photovoltaic performances. From the front view of the molecular geometries, it was clearly observed that the backbone of PQ4 is highly twisted but the other three polymers are more planar. The dihedral angle between thiophene and BDT is 24.2° for PQ4, which is larger than that in PQ1 (7.5°) PQ2 (6.8°) and PQ3 (8.3°). The reason could be attributed to the steric hindrance caused by the methyl side chain on thiophene units. Among these four polymers, PQ2 shows highest coplanarity which is beneficial for π - π stacking of its backbone in the solid state and charge transfer, which could result in higher photovoltaic performance of PQ2 based solar cells.

3.6. Photovoltaic properties, external quantum efficiency, and mobility

The bulk-heterojunction PSCs devices were made with a structure of ITO/PEDOT:PSS/Polymer:PCBM/Ca/Al as shown in Fig. 5(1). The driving force for the exciton dissociation is the energy level offset of LUMO (ΔE_1 in Fig. 5(1)) and HOMO (ΔE_3) between the donor (conjugated polymer) and acceptor (PCBM) materials. The V_{oc} is mainly related to the energy level offset (ΔE_2 in Fig. 5(1)) between the LUMO of the acceptor and the HOMO of the donor [42],

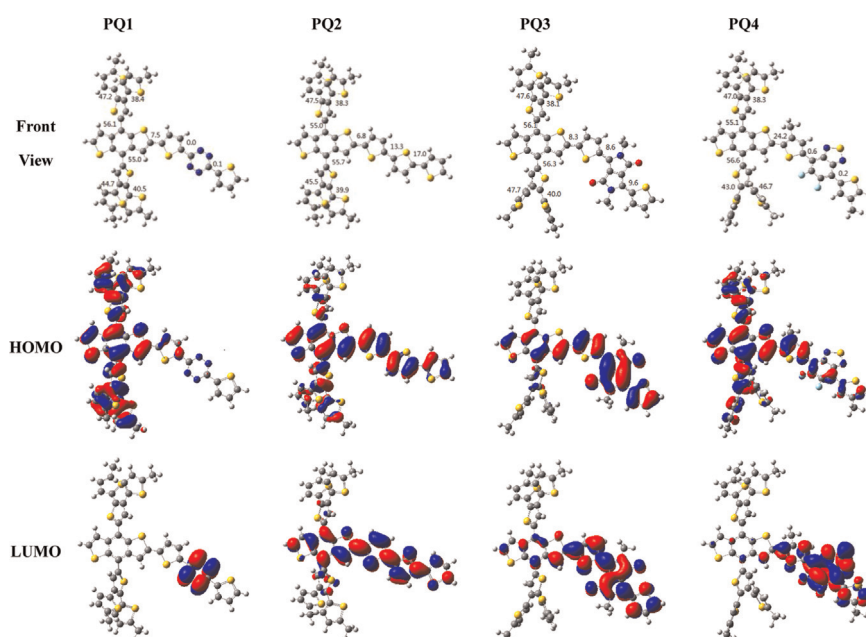


Fig. 4. The calculated HOMO and LUMO orbitals of the polymers and their molecular geometries from front view.

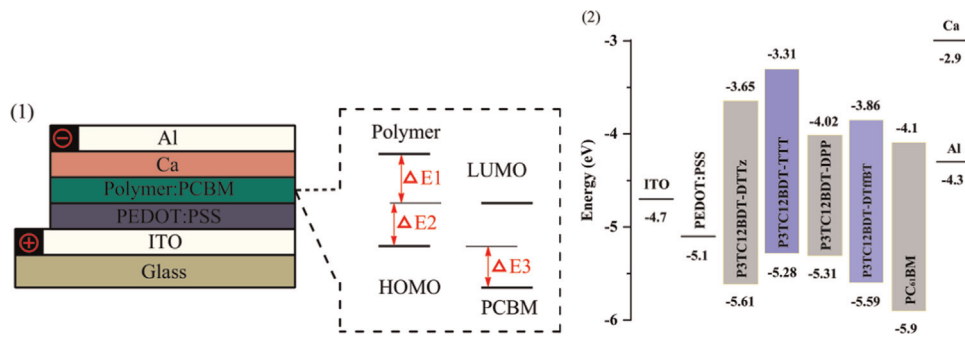


Fig. 5. (1) Schematic diagram of PSCs devices. (2) Electronic energy levels of materials used in PSCs devices.

Table 3
PSCs devices performances

Polymers	Ratio	V _{oc} (V)	J _{sc} (mA/cm ²)	FF(%)	PCE(%)	Spin speed (rpm)	Thickness (nm)
PQ1	1:2 ^a	0.98	2.18	42.03	0.90	800	133
PQ1	1:3^a	1.01	2.12	50.68	1.08	1000	75
PQ1	1:4 ^a	0.98	1.98	53.36	1.03	1000	96
PQ1	1:3 ^b	0.86	2.37	37.47	0.77	1200	81
PQ1	1:3 ^{b,c}	0.87	2.36	39.04	0.80	1200	81
PQ2	1:1 ^a	0.74	5.31	41.82	1.64	1500	107
PQ2	1:1.5 ^a	0.83	7.06	58.43	3.41	2000	81
PQ2	1:2 ^a	0.81	5.75	66.47	3.08	1500	113
PQ2	1:1.5 ^b	0.82	7.72	56.10	3.54	2000	85
PQ2	1:1.5^{b,c}	0.80	7.68	62.05	3.80	2000	85
PQ3	1:1.5 ^a	0.75	1.47	48.74	0.54	1000	89
PQ3	1:2 ^a	0.75	1.47	53.67	0.59	1000	93
PQ3	1:2.5 ^a	0.76	1.19	58.15	0.53	800	103
PQ3	1:2 ^b	0.77	2.35	56.55	1.02	1000	96
PQ3	1:2^{b,c}	0.78	2.67	52.36	1.09	1000	96
PQ4	1:5:1 ^a	0.83	4.20	43.22	1.52	1000	82
PQ4	1:1 ^a	0.90	4.57	49.63	2.04	800	106
PQ4	1:1.5 ^a	0.89	3.96	47.48	1.67	600	152
PQ4	1:1^b	0.94	6.17	48.80	2.83	800	112
PQ4	1:1 ^{b,c}	0.92	5.84	50.38	2.70	800	112

^a Polymer:PC₆₁BM.

^b Polymer:PC₇₁BM.

^c Annealing at 90 °C for 10 min.

46, 47]. Fig. 5(2) shows the electronic energy levels of materials used in PSCs devices. The active layers were prepared in the solutions of *o*-DCB with the concentration of 24 mg/mL (polymer:PCBM/*o*-DCB). Different spin speeds were used to control the thickness of the active layers. First, a series of D/A (polymer:PC₆₁BM, w/w) ratios were scanned from 1:1 to 1:4 to decide the optimum D/A ratio for each polymer that gave the best solar cell performances. The current density–voltage (*J*–*V*) curves are provided in Supporting information (Fig. S5), and the detailed data are collected in Table 3. It shows that the optimum D/A ratio for the PQ1:PC₆₁BM, PQ2:PC₆₁BM, PQ3:PC₆₁BM and PQ4:PC₆₁BM blends are 1:3, 1:1.5, 1:2, and 1:1, respectively. The different optimum D/A ratios of these four polymers might be attributed to the LUMO and HOMO electron distribution difference (Fig. 4 DFT results). For the devices based on PQ1:PC₆₁BM and PQ3:PC₆₁BM, low PCEs of 1.08% for PQ1 (*V*_{oc}=1.01 V, *J*_{sc}=2.12 mA/cm², FF=50.68%) and 0.59% for PQ3 (*V*_{oc}=0.75 V, *J*_{sc}=1.47 mA/cm², FF=53.67%) are achieved. The low PCEs of these two polymers were mainly caused by the low short-circuit current density (*J*_{sc}) which could be related to the energy level offset of LUMO between the donor and acceptor materials. Because the driving force for the exciton dissociation is the energy level offset of LUMO between the donor and acceptor materials, a minimum offset of approximately 0.3–0.4 eV is necessary to ensure efficient exciton dissociation at the D/A interface [42,46,47]. The relative low *J*_{sc} of the PSCs device could also partly due to the moderate absorption coefficients (Fig. S4).

After D/A ratios optimization, the best PCEs of the devices based on PQ2 and PQ4 are 3.41% and 2.04%, respectively. Furthermore, instead of PC₆₁BM, PC₇₁BM is used to tune the energy level matching degree. Highest PCEs of 2.83% for PQ4 and PC₇₁BM based devices are achieved. Thermal annealing is used to further enhance photovoltaic performance of the devices. Herein, devices based on polymers and PC₇₁BM with the optimum D/A ratios are thermal annealed at different temperatures for 10 min before cathode evaporation. The *J*–*V* curves and data of the PSCs devices are provided in Supporting Information (Figs. S6 and S7 and Table S1), and the best photovoltaic results are shown in Table 3 and Fig. 6. Finally, highest PCEs of 3.80% for PQ2 and PC₇₁BM based devices are achieved after thermal annealing at 90 °C for 10 min.

For polymer PQ1, PQ2, PQ3 and PQ4, the detailed photovoltaic performances are compared with these of the polymers which have the same backbone structure but do not have the bulky terthiophene side chain (PBDT-TTz [48], PBDT-1T-TTz [49], PBT-3T [50], PDPP-BDT [26], and PBDT_{TEH}-DT_HBTff [34]). Compared with PQ1, PBDT-TTz is kind of polymer with the same backbone but not 2D side-chain, and polymer PBDT-1T-TTz also has the same backbone but with typically 2D alkylthienyl side-chain. From the detailed optical-electronic properties and PSCs devices performances listed in Table 4, when BDT is copolymerized with DTTz segment, our bulky side group (terthiophene) does help for high *V*_{oc} devices. For PQ2 and PBT-3T, PQ2 shows relative high *E*_g and *V*_{oc}, and the *E*_g–*eV*_{oc} is similar. For polymer PQ3 (compared with PDPP-BDT) and PQ4 (compared with PBDT_{TEH}-DT_HBTff), PQ3 and PQ4 show almost the same *E*_g with PDPP-BDT and PBDT_{TEH}-DT_HBTff, but much higher *V*_{oc} and much lower *E*_g–*eV*_{oc} (Table 4). To highlight the high *V*_{oc} feature of devices, researchers define the donor photon energy loss as *E*_g–*eV*_{oc}, where *E*_g is the optical band gap of the donor polymer and *V*_{oc} is obtained from the corresponding device with either PC₆₁BM or PC₇₁BM [51]. Especially, we note that PQ3 shows *E*_g–*eV*_{oc}=0.51, which is almost the lowest *E*_g–*eV*_{oc} value achieved by researchers up to now [51,52]. This indicates that PQ3 is such a good photovoltaic polymer that can produce *V*_{oc}~0.78 V with a low *E*_g~1.29 eV. From Table 4, we can conclude that the bulky terthiophene side group helps to improve *V*_{oc} of the PSCs devices.

External quantum efficiency (EQE) curves based on the four polymers prepared through the optimum fabrication processes are shown in Fig. 6. As shown, the devices based on PQ1, PQ2, PQ4 possess a broad response range covering from 300 to 800 nm, and EQE peak values of the PSCs are 18.62%, 59.14%, and 42.79% respectively. Although the PSC device of PQ3 owns a more broad response range covering from 300 to 900 nm, but the EQE peak value is 17.07% only. The EQE values of the PSCs based on the four polymers agree with the *J*_{sc} of the corresponding devices. The high EQE values of the devices in 350–500 nm should result from the strong absorption of PCBM. The hole mobilities of the devices based on the four polymers are 1.86×10^{-7} , 1.84×10^{-5} , 2.21×10^{-5} , and

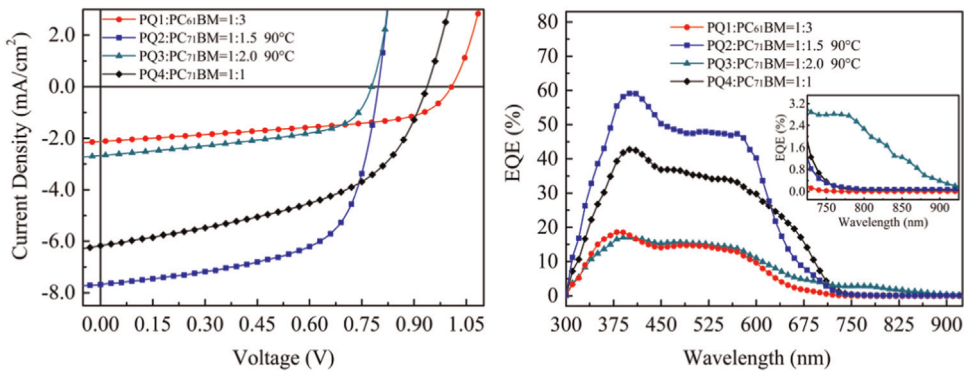


Fig. 6. J - V and EQE curves of the optimum devices based on these four polymers.

Table 4

Comparison photovoltaic properties of PSCs devices of PQ1, 2, 3 and 4 with analogs.

Polymer(D)	Acceptor(A)	D:A(w/w)	E_g (eV)	V_{oc} (V)	$E_g - eV_{oc}$ (eV)	J_{sc} (mA/cm ²)	FF(%)	PCE(%)	Ref.
PQ1	PC ₆₁ BM	1:3	1.96	1.01	0.95	2.12	56	1.08	This work
PQ1	PC ₇₁ BM	1:3	1.96	0.87	1.09	2.36	39.04	0.80	This work
PBDT-TTz	PC ₇₁ BM	1:3	1.85	0.92	0.93	6.21	58	3.32	[48]
PBDT-1T-TTz	PC ₇₁ BM	1:1	1.93	0.92	1.01	8.02	40.9	3.0	[49]
PQ2	PC ₆₁ BM	1:2	1.97	0.81	1.16	5.75	66.47	3.08	This work
PBT-3T	PC ₆₁ BM	1:3	1.65	0.47	1.18	2.15	34	0.34	[50]
PQ3	PC ₇₁ BM	1:2	1.29	0.78	0.51	2.67	52.36	1.09	This work
PDPP-BDT	PC ₇₁ BM	1:2	1.31	0.68	0.63	8.40	44.3	2.53	[26]
PQ4	PC ₇₁ BM	1:1.5	1.73	0.89	0.84	3.96	47.48	1.67	This work
PBDT _{TEH} -DT _H BTff	PC ₇₁ BM	1:1.5	1.72	0.68	1.04	11.87	55.2	4.46	[34]

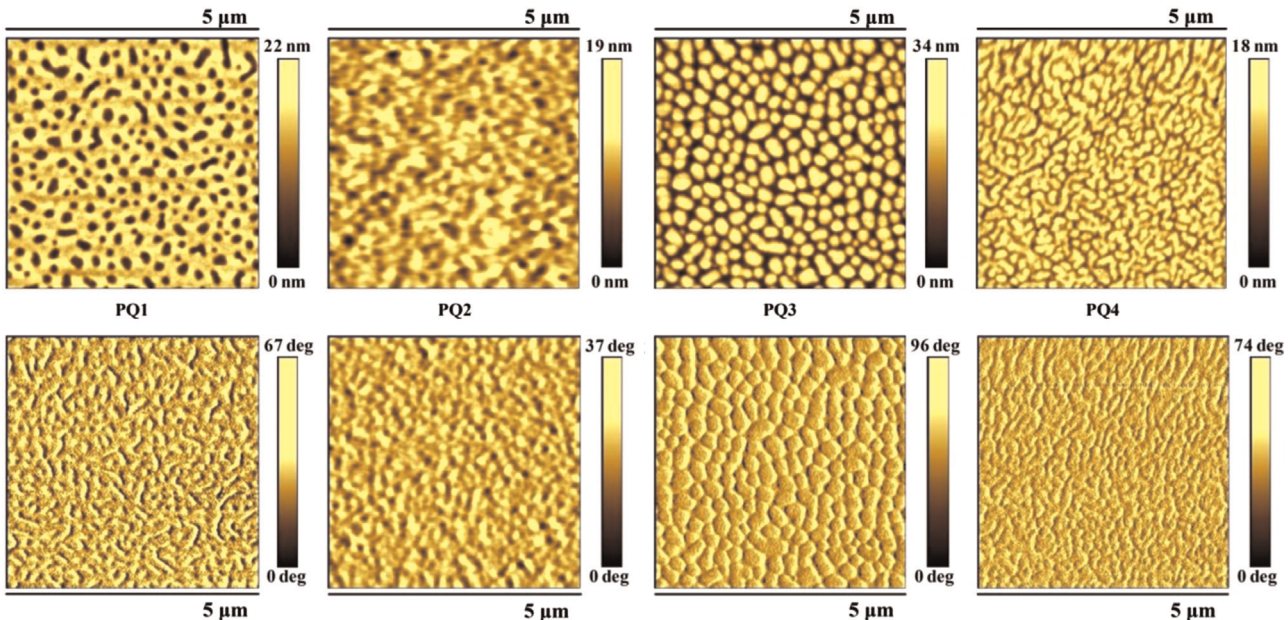


Fig. 7. AFM height (up) and phase images (down) of blend films of polymers/PCBM processed under optimum conditions.

5.86×10^{-6} cm²/Vs respectively (Fig. S8), measured by the space-charge limit current (SCLC) method with a device structure of ITO/PEDOT:PSS/Polymer:PCBM/Au. The low hole mobilities are possibly caused by the bulky terthiophene side group and the long alkyl chain induced polymer backbone twist which make the polymer difficult to pack and crystallization. The hole mobilities of PQ1, PQ2, and PQ4 are consistent with the PCEs values. PQ3 shows the highest one among the four polymers, indicating that PQ3 would have no

serious shortage in charge transport, so that we suspected that the blend of PQ3:PCBM may have serious problems in morphologies.

3.7. Morphology and XRD

Nanoscale surface morphologies of the blend films processed with the optimum conditions were investigated by the atomic force microscope (AFM) (Fig. 7). The root-mean-square roughness (R_q) values obtained from the height image were 10.1, 3.95, 13.5 and

7.73 nm for the blends of PQ1–PQ4, respectively. From the imagines, we can obviously observe that PQ1 and PCBM cannot form good interpenetrating network structure. PQ3 shows large domain size over 250 nm which is detrimental to get efficient exciton dissociation. This explains why the EQE response values and the J_{sc} of devices based on PQ3 are miserably low. PQ2 and PQ4 exhibits better interpenetrating network structure and smooth interface which lead to higher PCEs of devices based on this two polymers. From the X-ray diffraction (Fig. S9), four polymers appeared to be amorphous as there were no obvious peaks in the XRD spectra either the pure polymers or the blend films with PCBM.

4. Conclusions

In this work, four benzodithiophene (BDT) copolymers based on bulky terthiophene side chain substitutes were designed and synthesized. Due to the difference in electron affinity of acceptor units, these four polymers show different optical band gaps (1.3–2 eV), but they all remain deep HOMO energy levels (−5.3 to 5.6 eV) probably partially due to the bulky terthiophene side chain effect. Compared with the polymer photovoltaic properties in the literature which have the same polymer backbone but do not have the bulky terthiophene side group, it can be concluded that the bulky terthiophene side group does help to improve V_{oc} of the PSCs devices. The moderate devices performances is due to the relatively low J_{sc} which is limited by the molecule geometry, hole mobility and active layer morphology. Further work to utilize the bulky terthiophene side chain to synthesize highly efficient BDT polymer solar cells donor is underway.

Acknowledgments

This work was supported by the NSFC (21274134, 21274161, 51173199, 61107090), New Century Excellent Talents in University (NCET-11-0473), and Ministry of Science and Technology of China (2014CB643501, 2010DFA52310).

Appendix A. Supplementary information

Supplementary data associated with this article can be found in the online version at <http://dx.doi.org/10.1016/j.solmat.2015.02.022>.

References

- [1] J. Chen, Y. Cao, Development of novel conjugated donor polymers for high-efficiency bulk-heterojunction photovoltaic devices, *Acc. Chem. Res.* 42 (2009) 1709–1718.
- [2] W.-H. Lee, S.K. Son, K. Kim, S.K. Lee, W.S. Shin, S.-J. Moon, I.-N. Kang, Synthesis and characterization of new selenophene-based donor-acceptor low-bandgap polymers for organic photovoltaic cells, *Macromolecules* 45 (2012) 1303–1312.
- [3] N.S. Sariciftci, L. Smilowitz, A.J. Heeger, F. Wudl, Photoinduced electron transfer from a conducting polymer to buckminsterfullerene, *Science* 258 (1992) 1474–1476.
- [4] G. Yu, J. Gao, J.C. Hummelen, F. Wudl, A.J. Heeger, Polymer photovoltaic cells: enhanced efficiencies via a network of internal donor–acceptor heterojunctions, *Science* 270 (1995) 1789–1790.
- [5] J. Peet, A.J. Heeger, G.C. Bazan, “Plastic” solar cells: self-assembly of bulk heterojunction nanomaterials by spontaneous phase separation, *Acc. Chem. Res.* 42 (2009) 1700–1708.
- [6] H. Pan, Y. Li, Y. Wu, P. Liu, B.S. Ong, S. Zhu, G. Xu, Low-temperature, solution-processed, high-mobility polymer semiconductors for thin-film transistors, *J. Am. Chem. Soc.* 129 (2007) 4112–4113.
- [7] H. Pan, Y. Li, Y. Wu, P. Liu, B.S. Ong, S. Zhu, G. Xu, Synthesis and thin-film transistor performance of poly(4,8-didodecylbenzo[1,2-*b*:4,5-*b'*]dithiophene), *Chem. Mater.* 18 (2006) 3237–3241.
- [8] J. Hou, M.-H. Park, S. Zhang, Y. Yao, L.-M. Chen, J.-H. Li, Y. Yang, Bandgap and molecular energy level control of conjugated polymer photovoltaic materials based on benzo[1,2-*b*:4,5-*b'*]dithiophene, *Macromolecules* 41 (2008) 6012–6018.
- [9] X. Sun, W. Chen, Z. Du, X. Bao, G. Song, K. Guo, N. Wang, R. Yang, Synthesis and photovoltaic properties of novel 3,4-ethylenedithiophene-based copolymers for organic solar cells, *Polym. Chem.* 4 (2013) 1317–1322.
- [10] Z. Ma, E. Wang, M.E. Jarvid, P. Henriksson, O. Inganäs, F. Zhang, M.R. Andersson, Synthesis and characterization of benzodithiophene-iso-indigo polymers for solar cells, *J. Mater. Chem.* 22 (2012) 2306–2314.
- [11] V. Manninen, M. Niskanen, T.I. Hukka, F. Pasker, S. Claus, S. Höger, J. Baek, T. Umeyama, H. Imahori, H. Lemmyinen, Conjugated donor–acceptor (D–A) copolymers in inverted organic solar cells—a combined experimental and modelling study, *J. Mater. Chem. A* 1 (2013) 7451–7462.
- [12] D. Kotowski, S. Luzzati, G. Bianchi, A. Calabrese, A. Pellegrino, R. Po, G. Schimperna, A. Tacca, Double acceptor D–A copolymers containing benzotriazole and benzothiadiazole units: chemical tailoring towards efficient photovoltaic properties, *J. Mater. Chem. A* 1 (2013) 10736–10744.
- [13] H.-Y. Chen, J. Hou, S. Zhang, Y. Liang, G. Yang, Y. Yang, L. Yu, Y. Wu, G. Li, Polymer solar cells with enhanced open-circuit voltage and efficiency, *Nat. Photonics* 3 (2009) 649–653.
- [14] J. Hou, H.-Y. Chen, S. Zhang, R.J. Chen, Y. Yang, Y. Wu, G. Li, Synthesis of a low band gap polymer and its application in highly efficient polymer solar cells, *J. Am. Chem. Soc.* 131 (2009) 15586–15587.
- [15] Y. Liang, L. Yu, A new class of semiconducting polymers for bulk heterojunction solar cells with exceptionally high performance, *Acc. Chem. Res.* 43 (2010) 1227–1236.
- [16] C. Piliego, T.W. Holcombe, J.D. Douglas, C.H. Woo, P.M. Beaujuge, J.M.J. Fréchet, Synthetic control of structural order in N-alkylthieno[3,4-*c*]pyrrole-4,6-dione-based polymers for efficient solar cells, *J. Am. Chem. Soc.* 132 (2010) 7595–7597.
- [17] C. Cabanatos, A. El Labban, J.A. Bartelt, J.D. Douglas, W.R. Mateker, J.M. Fréchet, M.D. McGehee, P.M. Beaujuge, Linear side chains in benzo[1,2-*b*:4,5-*b'*]dithiophene-thieno[3,4-*c*]pyrrole-4,6-dione polymers direct self-assembly and solar cell performance, *J. Am. Chem. Soc.* 135 (2013) 4656–4659.
- [18] L. Huo, J. Hou, Benzo[1,2-*b*:4,5-*b'*]dithiophene-based conjugated polymers: band gap and energy level control and their application in polymer solar cells, *Polym. Chem.* 2 (2011) 2453–2461.
- [19] J. Hou, Z. Tan, Y. Yan, Y. He, C. Yang, Y. Li, Synthesis and photovoltaic properties of two-dimensional conjugated polythiophenes with bi(thienylenevinylene) side chains, *J. Am. Chem. Soc.* 128 (2006) 4911–4916.
- [20] Y. Li, Y. Zou, Conjugated polymer photovoltaic materials with broad absorption band and high charge carrier mobility, *Adv. Mater.* 20 (2008) 2952–2958.
- [21] L. Huo, J. Hou, S. Zhang, H.-Y. Chen, Y. Yang, A polybenzo[1,2-*b*:4,5-*b'*]dithiophene derivative with deep HOMO level and its application in high-performance polymer solar cells, *Angew. Chem. Int. Ed.* 49 (2010) 1500–1503.
- [22] L. Huo, S. Zhang, X. Guo, F. Xu, Y. Li, J. Hou, Replacing alkoxy groups with alkylthienyl groups: a feasible approach to improve the properties of photovoltaic polymers, *Angew. Chem.* 123 (2011) 9871–9876.
- [23] R. Duan, L. Ye, X. Guo, Y. Huang, P. Wang, S. Zhang, J. Zhang, L. Huo, J. Hou, Application of two-dimensional conjugated benzo[1,2-*b*:4,5-*b'*]dithiophene in quinoxaline-based photovoltaic polymers, *Macromolecules* 45 (2012) 3032–3038.
- [24] S. Zhang, L. Ye, Q. Wang, Z. Li, X. Guo, L. Huo, H. Fan, J. Hou, Enhanced photovoltaic performance of diketopyrrolopyrrole (DPP)-based polymers with extended π conjugation, *J. Phys. Chem. C* 117 (2013) 9550–9557.
- [25] L. Dou, J. Gao, E. Richard, J. You, C.-C. Chen, K.C. Cha, Y. He, G. Li, Y. Yang, Systematic investigation of benzodithiophene- and diketopyrrolopyrrole-based low-bandgap polymers designed for single junction and tandem polymer solar cells, *J. Am. Chem. Soc.* 134 (2012) 10071–10079.
- [26] L. Huo, J. Hou, H.-Y. Chen, S. Zhang, Y. Jiang, T.L. Chen, Y. Yang, Bandgap and molecular level control of the low-bandgap polymers based on 3,6-dithiophen-2-yl-2,5-dihydropyrrolo[3,4-*c*]pyrrole-1,4-dione toward highly efficient polymer solar cells, *Macromolecules* 42 (2009) 6564–6571.
- [27] M. Zhang, Y. Gu, X. Guo, F. Liu, S. Zhang, L. Huo, T.P. Russell, J. Hou, Efficient polymer solar cells based on benzothiadiazole and alkylphenyl substituted benzodithiophene with a power conversion efficiency over 8%, *Adv. Mater.* 25 (2013) 4944–4949.
- [28] Y. Huang, F. Liu, X. Guo, W. Zhang, Y. Gu, J. Zhang, C.C. Han, T.P. Russell, J. Hou, Manipulating backbone structure to enhance low band gap polymer photovoltaic performance, *Adv. Energy Mater.* 3 (2013) 930–937.
- [29] L. Ye, S. Zhang, L. Huo, M. Zhang, J. Hou, Molecular design toward highly efficient photovoltaic polymers based on two-dimensional conjugated benzodithiophene, *Acc. Chem. Res.* 47 (2014) 1595–1603.
- [30] C.-Q. Ma, E. Mena-Osteritz, T. Debaerdemaecker, M.M. Wienk, R.A.J. Janssen, P. Bäuerle, Functionalized 3D oligothiophene dendrons and dendrimers—novel macromolecules for organic electronics, *Angew. Chem.* 119 (2007) 1709–1713.
- [31] Q. Liu, X. Bao, S. Wen, Z. Du, L. Han, D. Zhu, Y. Chen, M. Sun, R. Yang, Hyper-conjugated side chained benzodithiophene and 4,7-di-2-thienyl-2,1,3-benzothiadiazole based polymer for solar cells, *Polym. Chem.* 5 (2014) 2076–2082.
- [32] M. Zhang, X. Guo, X. Wang, H. Wang, Y. Li, Synthesis and photovoltaic properties of D–A copolymers based on alkyl-substituted indacenodithiophene donor unit, *Chem. Mater.* 23 (2011) 4264–4270.
- [33] K.H. Hendriks, G.H.L. Heintges, V.S. Gevaerts, M.M. Wienk, R.A.J. Janssen, High-molecular-weight regular alternating diketopyrrolopyrrole-based terpolymers for efficient organic solar cells, *Angew. Chem. Int. Ed.* 52 (2013) 8341–8344.
- [34] N. Wang, Z. Chen, W. Wei, Z. Jiang, Fluorinated benzothiadiazole-based conjugated polymers for high-performance polymer solar cells without any

- processing additives or post-treatments, *J. Am. Chem. Soc.* 135 (2013) 17060–17068.
- [35] C.F.N. Marchiori, N.A.D. Yamamoto, I.R. Grova, A.G. Macedo, M. Paulus, C. Sternemann, S. Huotari, L. Akcelrud, L.S. Roman, M. Koehler, Performance of fluorene and terthiophene copolymer in bilayer photovoltaic devices: the role of the polymer conformations, *Org. Electron.* 13 (2012) 2716–2726.
- [36] P. Sista, H. Nguyen, J.W. Murphy, J. Hao, D.K. Dei, K. Palaniappan, J. Servello, R.S. Kularatne, B.E. Gnade, B. Xue, P.C. Dastoor, M.C. Biewer, M.C. Stefan, Synthesis and electronic properties of semiconducting polymers containing benzodithiophene with alkyl phenylethynyl substituents, *Macromolecules* 43 (2010) 8063–8070.
- [37] P.M. Beaujuge, C.M. Amb, J.R. Reynolds, Spectral engineering in π -conjugated polymers with intramolecular donor–acceptor interactions, *Acc. Chem. Res.* 43 (2010) 1396–1407.
- [38] Y. Zou, A. Najari, P. Berrouard, S. Beaupré, B.R. Aich, Y. Tao, M. Leclerc, A thieno [3,4-c] pyrrole-4,6-dione-based copolymer for efficient solar cells, *J. Am. Chem. Soc.* 132 (2010) 5330–5331.
- [39] P.J. Brown, D.S. Thomas, A. Köhler, J.S. Wilson, J.-S. Kim, C.M. Ramsdale, H. Sirringhaus, R.H. Friend, Effect of interchain interactions on the absorption and emission of poly (3-hexylthiophene), *Phys. Rev. B* 67 (2003) 064203.
- [40] L. Dou, J. You, J. Yang, C.-C. Chen, Y. He, S. Murase, T. Moriarty, K. Emery, G. Li, Y. Yang, Tandem polymer solar cells featuring a spectrally matched low-bandgap polymer, *Nat. Photonics* 6 (2012) 180–185.
- [41] Y. Li, Y. Cao, J. Gao, D. Wang, G. Yu, A.J. Heeger, Electrochemical properties of luminescent polymers and polymer light-emitting electrochemical cells, *Synth. Met.* 99 (1999) 243–248.
- [42] M.C. Scharber, D. Mühlbacher, M. Koppe, P. Denk, C. Waldauf, A.J. Heeger, C.J. Brabec, Design rules for donors in bulk-heterojunction solar cells—towards 10% energy-conversion efficiency, *Adv. Mater.* 18 (2006) 789–794.
- [43] C. Lee, W. Yang, R.G. Parr, Development of the colle-salvetti correlation-energy formula into a functional of the electron density, *Phys. Rev. B* 37 (1988) 785.
- [44] A.D. Becke, Density-functional thermochemistry. III. The role of exact exchange, *J. Chem. Phys.* 98 (1993) 5648–5652.
- [45] W.J. Hehre, R. Ditchfield, J.A. Pople, Self-consistent molecular orbital methods. XII. Further extensions of Gaussian-type basis sets for use in molecular orbital studies of organic molecules, *J. Chem. Phys.* 56 (1972) 2257–2261.
- [46] A. Mishra, P. Bäuerle, Small molecule organic semiconductors on the move: promises for future solar energy technology, *Angew. Chem. Int. Ed.* 51 (2012) 2020–2067.
- [47] Y. Li, Molecular design of photovoltaic materials for polymer solar cells: toward suitable electronic energy levels and broad absorption, *Acc. Chem. Res.* 45 (2012) 723–733.
- [48] S. Wen, Q. Dong, W. Cheng, P. Li, B. Xu, W. Tian, A benzo [1,2-b:4,5-b'] dithiophene-based copolymer with deep HOMO level for efficient polymer solar cells, *Sol. Energy Mater. Sol. Cells* 100 (2012) 239–245.
- [49] W. Cheng, Z. Wu, S. Wen, B. Xu, H. Li, F. Zhu, W. Tian, Donor–acceptor copolymers incorporating polybenzo [1,2-b:4,5-b'] dithiophene and tetrazine for high open circuit voltage polymer solar cells, *Org. Electron.* 14 (2013) 2124–2131.
- [50] E. Lim, S. Lee, K.K. Lee, Synthesis and photovoltaic properties of new conjugated polymers based on benzo [1,2-b:4,5-b'] dithiophene, *J. Nanosci. Nanotechnol.* 12 (2012) 4243–4247.
- [51] M. Wang, H. Wang, T. Yokoyama, X. Liu, Y. Huang, Y. Zhang, T.-Q. Nguyen, S. Aramaki, G.C. Bazan, High open circuit voltage in regioregular narrow bandgap polymer solar cells, *J. Am. Chem. Soc.* 136 (2014) 12576–12579.
- [52] J.W. Jung, J.W. Jo, F. Liu, T.P. Russell, W.H. Jo, A low band-gap polymer based on unsubstituted benzo [1,2-b:4,5-b'] dithiophene for high performance organic photovoltaics, *Chem. Commun.* 48 (2012) 6933–6935.